PLATFORM - A Journal of Science & Technology

Received: 1 May 2021, Accepted: 29 July 2021, Published: 30 November 2021, Publisher: UTP Press, Creative Commons: CC BY-NC-ND 4.0

TUNGSTEN OXIDE DOPED TITANIA SUPPORTED ON TUD-C FOR PHOTOCATALYTIC REMOVAL OF METHYLENE BLUE

Chui Min Ling[1], Chin Chai Teng[1], Mohd Hayrie Mohd Hatta[1,3], Siew Ling Lee[1,2*]

[1]Department of Chemistry, Faculty of Science, Universiti Teknologi Malaysia
[2]Centre for Sustainable Nanomaterials, Ibnu Sina Institute for Scientific and Industrial Research, Universiti Teknologi Malaysia
[3]Centre of Research and Development, Asia Metropolitan University, Malaysia

*Email: lsling@utm.my

ABSTRACT

In this work, a series of mesoporous tungsten oxide (WO_3) doped titania (TiO_2) supported on Technische Universiteit Delft (TUD-C) (WO_3-TiO_2/TUD-C) were successfully prepared by the sol-gel method. X-ray diffraction (XRD) analysis showed that the samples' crystallinity decreased after incorporation of WO_3-TiO_2 onto TUD-C, suggesting the successful incorporating WO_3-TiO_2 into the framework of TUD-C. N_2 adsorption-desorption isotherm analysis indicated that the surface area, pore volume and pore size of WO_3-TiO_2/TUD-C increased significantly after loading onto TUD-C. The presence of tetrahedron frame structure Ti^{4+} and polytitanate in all the prepared samples were detected. Besides, all the WO_3-TiO_2 supported on TUD-C samples showed reduced band gap energy of 3.11 eV. The presence of zeolitic materials in the sample was confirmed by Fourier transform infrared spectroscopy, indicating the successfull formation of TUD-C. The Field Emission Scanning Electron Microsope (FESEM) images revealed the WO_3-TiO_2 were distributed uniformly on the surface of TUD-C. It has been demonstrated that the best photocatalytic activity for removal of methylene blue under UV light irradiation was achieved when WO_3-TiO_2/TUD-C was prepared with the molar ratio of Si to Ti is equal to 30 (WO_3-TiO_2/TUD-C(30)). The current research findings suggested that high pore size, surface area and crystallinity were the key factors for the high photocatalytic activity.

***Keywords**: Photocatalyst, titania, TUD-C, tungsten oxide, methylene blue*

INTRODUCTION

Since the historical period, natural dyes that are obtained from natural resources such as flowers, fruits, leaves, and barks, have been used as dyes for the colour purpose of textiles and clothes. Natural dyes are considered harmless and less expensive since they can be extracted from nature but their low quality and variety have limited their applications [1]. Therefore, the synthetic dyes have been highly demanded for the past 150 years [2].

Today's synthetic dyes have been practically and widely applied to give colour to paper, textiles, leather and other materials in conditions that the colouring reagent is not easily altered by washing or heat process or other causes that could lead the material to be exposed [1]-[3]. However, the synthetic dyes present in wastewater that are discharged from the textiles industry have led to the major problem in environmental pollution [3]-[4] as it can contaminate the soil and water bodies to create a serious ecological problem. According to the report, approximately 20% of dyes are lost as pollutants into soil or water during the operational process [4]. For example, methylene blue, commonly abbreviated as MB, is widely used as colouring reagent in textiles, chemical indicators, and biological dyes. This dye possesses properties such as high concentration in organic matter and poor biodegradability. Thus its presence has seriously affected the water system and photosynthesis reaction of microorganisms in the environment [3],[5]-[6]. Hence, the removal of

dyes in the wastewater are highly required in order to preserve the nature. Currently, there are several common methods available for the removal of dyes in wastewater, such as precipitation [7], adsorption [8], and flocculation [9]. However, the problem associated with these methods is the need for physicochemical monitoring of the effluent, increased in the generation of sludge volume, high cost in the preparation of material and less efficient with certain types of dyes [10].

Advance Oxidation Process (AOP) which is a safe, green, environmentally friendly and low-cost method, is a technology that uses hydroxyl radicals or oxidants to treat organic pollutants in wastewater [11]. By far, TiO_2 is widely recognized as a promising photocatalyst to solve the issues. The TiO_2 photocatalyst is proven to be chemically stable, harmless, and able to utilize light and air to form many reactive species, including the hydroxyl radicals, to degrade the harmful organic contaminants [12]. However, its large band gap (*ca.* 3.2 eV), high electron-hole recombination rate, and low surface area due to particles agglomeration have limited its photocatalytic performance [13]. Therefore, many researchers have reported the modifications of TiO_2 in order to enhance its photocatalytic activity, especially in improving the surface area and narrowing the band gap [12]-[13].

Many efforts were made to support TiO_2 onto high surface material such as mesoporous silica to improve the adsorbability of the materials, hence leading to better photocatalytic activity [13]-[15]. Recently, a mesoporous zeolitic material with a hierarchically structured composite with ZSM-5, namely TUD-C possesses a 3-D mesoporous matrix that forms a large surface area and well-separated pore size, which is suitable to act as support materials for metal oxides [16]-[17]. The TUD-C has an average high surface area of 1451 m^2/g with a pore volume of 0.73 cm^3/g [18]. In addition, its good thermal stability and three-dimensional (3-D) sponge-like silicate framework with high surface area and substrate accessibility make it advantageous for mesoporous and microporous materials [16]-[18]. It was reported that molybdena doped TiO_2 supported on TUD-C has successfully enhanced the surface area and pore size compared to molybdena doped TiO_2 alone [18]. On the other hand, others also report that different molar ratios of Si/Ti could have a significantly affect on the activity of the catalyst. The investigation on the molar ratio of Si/Ti showed that Cr doped TiO_2 with 30 ratios gave the highest activity [19].

As TiO_2 is commonly associated with high electron-hole recombination rates and wide band gap energy, doping with metal/metal oxide is highly suggested in order to overcome the present drawbacks [12]. Several reports have shown that doping with metal and metal oxide as well as nn metal compounds such as chromium, copper, and carbon have successfully reduced the band gap energy and electron-hole recombination rates [12]-[13],[20]-[22]. Recently, it was reported that the tungsten oxide (WO_3) modified TiO_2 showed higher activity compared to TiO_2 alone due to the existence of surface redox sites upon addition of WO_3 [23].

In this work, the WO_3 modified with TiO_2 supported on TUD-C was prepared via a combination of sol-gel and hydrothermal methods. The effect of differences Si/Ti molar ratios towards properties and activity of the resulting materials was investigated. The photocatalytic performance of WO_3-TiO_2/TUD-C was evaluated by removing methylene blue under UV light irradiation.

EXPERIMENTAL

Photocatalysts Preparation Synthesis of WO_3-TiO_2

WO_3-TiO_2 was prepared using the sol-gel method as reported previously [20]. At first, the titanium tetraisopropoxide, TTIP (Sigma Aldrich, 97%) was added to ethanol (Merck, 95%) and chelating agent, acetylacetone (Sigma Aldrich, 99.9%) according to the molar ratio of 1: 100: 2 followed by stirring for 1 h at room temperature. Ammonium tungstate (Sigma Aldrich, 99.9%) was added drop-wise into the solution in a continuous stirring for 1 h under evaporating solvent at 353 K. Finally, the sample was further dried overnight at 383 K followed by calcination time at 773 K for 5 h.

Synthesis of WO_3-TiO_2/TUD-C(x)

TUD-C was prepared by mixing water, tetraethyl orthosilicate (TEOS), triethanolamine (TEA) and ZSM-5 [23]. Tetraethylammonium hydroxide (TEAOH) was added dropwise to the mixture with continuous

stirring until gelation of the mixture was formed. The molar composition of synthesized TUD-C was set to TEOS: 1, ZSM-5: 0.5, TEA: 0.1, TEAOH: 11 H_2O. The formed solid gel was then dried at 373 K for 1-2 h followed by calcination at 873 K for 6 h. Prior to the addition of TEA and TEAOH, TEOS was added with distilled water while stirring with solid WO_3-TiO_2. The TUD-C(x) were prepare with 'x' representing different molar ratios of Si/Ti (10, 30 and 50).

Samples Characterizations

For structural analysis, all the prepared materials were characterized using Bruker Advance D8 X-ray diffractometer with Cu K_a radiation (λ = 1. 5406 Å) at 40 kV and 40 mA. The functional group analysis was performed using Thermo Scientific Nicolet iS50 spectrophotometer with potassium bromide (KBr) method, while the optical analysis was performed using Shimadzu UV-2600 for diffuse reflectance UV-Vis spectroscopy. Barium sulfate ($BaSO_4$) was used as the reference material prior to the measurement. The surface area and pore size analysis were conducted at 77 K using Thermo Fischer Scientific Sorptomatic 1990. Prior to the measurement, the sample was degassed at 523 K for 16 h Field emission scanning electron microscopy and energy-dispersive X-ray spectroscopy (EDX) analyses were used to characterise the photocatalysts' surface morphology and elemental mapping, respectively. The samples were scanned with JEOL JSM-6710F with a maximum 15 kV and 2 nA probe current.

Photocatalytic Test

A 0.1 g of prepared sample was added into the 100 mL beaker containing methylene blue solution (50 mL, 200 ppm). Prior to the photocatalytic testing, all the suspended samples in methylene blue solution were stirred in the dark condition for 1 h to achieve equilibrium. The reaction was performed using a UV light source (UVLS-28EL Series UV Lamp 8 W) for 1 h. Upon completion, the solution was filtered to obtain the sample. The final concentration of the solution was calculated by using UV-Visible spectroscopy. The final concentration of methylene blue was calculated using the ratio of removed methylene blue to its initial concentration as given by:

$$\text{Removal percentage} = \frac{A_o - A}{A_o} \times 100\% \quad (1)$$

A_o = Concentration after 1 h dark reaction
A = Concentration after 1 h light reaction

RESULTS AND DISCUSSION

Structural Analysis

Figure 1 illustrates the XRD spectra of prepared photocatalyst (a) WO_3-TiO_2, (b) TUD-C, (c) WO_3-TiO_2/TUD-C(10), (d) WO_3-TiO_2/TUD-C(30) and (e) WO_3-TiO_2/TUD-C(50). Based on the XRD patterns of WO_3-TiO_2, it was confirmed that TiO_2 in the prepared samples was present in the anatase phase [JCPDF 00-21-1272] with peaks clearly observed at 2θ of 25.30°, 36.95°, 37.79°, 38.57°, 48.03°, 53.89° and 55.06°. The formation of anatase phase in TiO_2 as observed in the XRD spectra was also in agreement with the XRD analysis of anatase TiO_2 as have been reported in previous literature [20]-[23]. The successful formation of TUD-C can be confirmed by the presence of the two sharp peaks at 2θ of 7.93°, 8.88°, assigned to aluminium silicate resembling silicate 1 (MFI) framework [24]. In addition, the peaks at 2θ of 23.05° and 23.30° are denoted as ZSM-5 zeolite [JCPDF 00-44-0003]. It can be seen that the modification of TiO_2 with WO_3 has significantly affected the crystallinity of TiO_2. The reduced crystallinity as shown in Figure 1(c) could be due to the successfu incorporation of WO_3 into TiO_2 [18]. Amongst the WO_3-TiO_2/TUD-C samples, the highest crystallinity was displayed by WO_3-TiO_2/TUD-C(30).

Optical Analysis

The optical properties of the prepared samples are presented in Figure 2. It was observed that all the spectra showed a predominant broad peak at 250 – 350 nm, indicating the formation of tetrahedron frame structure Ti^{4+} [18]-[20],[23]. The weak absorption at 400 nm and above showed that the amount of dopant was too low to give a noticeable effect on DR UV-Vis spectra. The presence of anatase TiO_2 can be confirmed at the wide peak at *ca.* 250 – 380 nm and it is in agreement with the results by XRD analysis. The band gap energy values of prepared samples were estimated using the Tauc plot as presented in Figure 3 and the values are shown in Table 1. The incorporation of WO_3 into TiO_2 has slightly decreased the band gap energy from 3.20 eV to 3.06 eV. However, the loading of TUD-C support to WO_3-TiO_2 has slightly increased the band gap energy to *ca.* 3.11 eV. On the other hand,

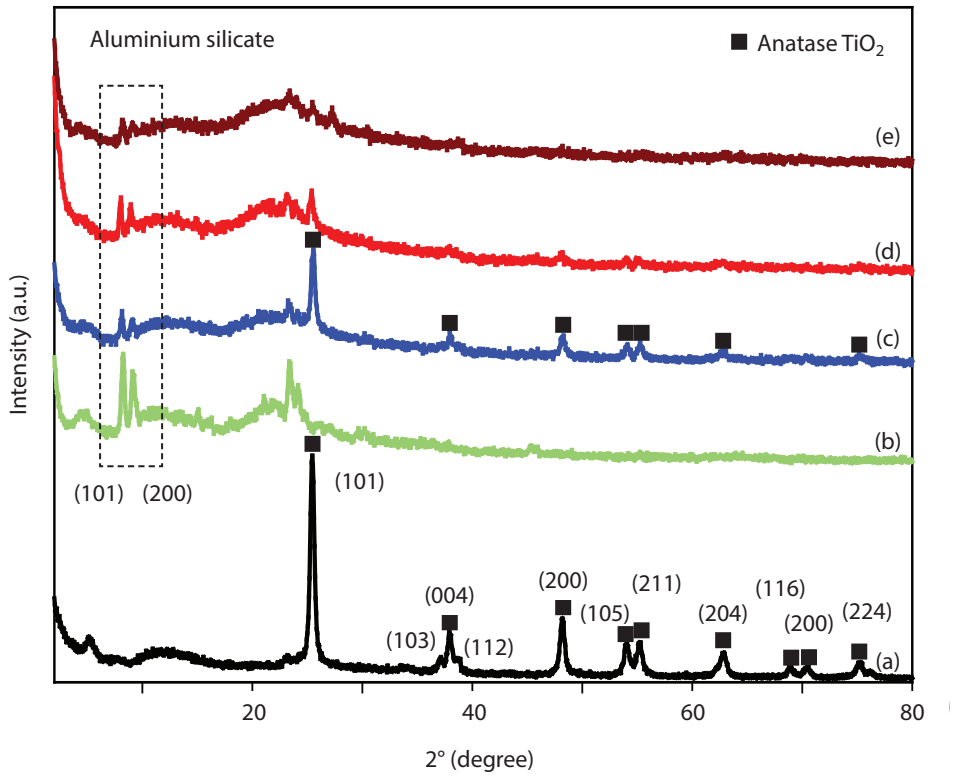

Figure 1 XRD patterns of (a) WO_3-TiO_2, (b) TUD-C, (c) WO_3-TiO_2/TUD-C(10), (d) WO_3-TiO_2/TUD-C(30), and (e) WO_3-TiO_2/TUD-C(50)

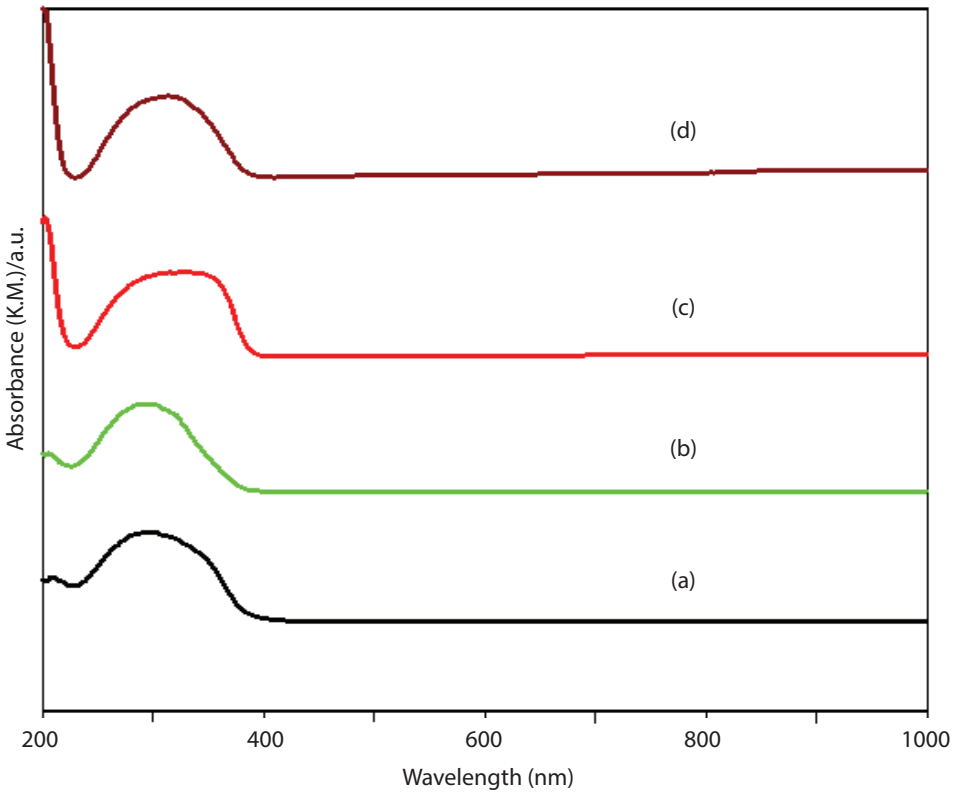

Figure 2 DR UV-Vis spectra of (a) WO_3-TiO_2, (b) WO_3-TiO_2/TUD-C(10), (c) WO_3-TiO_2/TUD-C(30) and (d) WO_3-TiO_2/TUD-C(50) samples

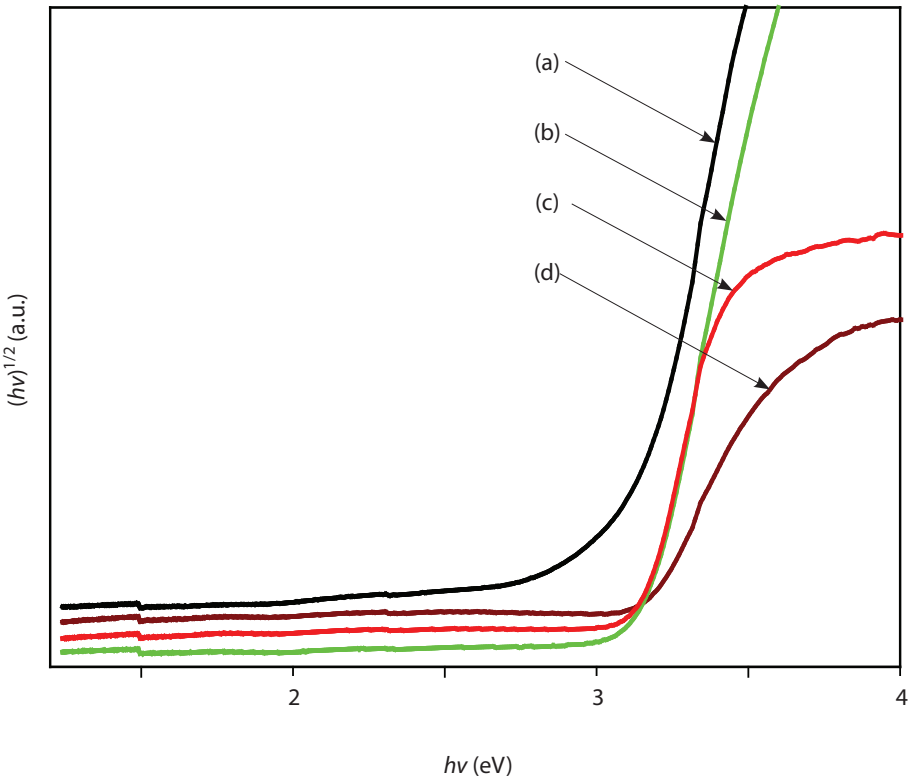

Figure 3 DR Tauc plot of (a) WO_3-TiO_2, (b) WO_3-TiO_2/TUD-C(10), (c) WO_3-TiO_2/TUD-C(30) and (d) WO_3-TiO_2/TUD-C(50) samples

Table 1 Band gap energy of WO_3 and WO_3-TiO_2 and WO_3-TiO_2/TUD-C(x)

Samples	Band gap energy (eV)
TiO_2[#]	3.20
WO_3-TiO_2	3.06
WO_3-TiO_2/TUD-C(10)	3.11
WO_3-TiO_2/TUD-C(30)	3.12
WO_3-TiO_2/TUD-C(50)	3.14

[#]The band gap value of TiO_2 was adapted from reported literatures [12],[13],[19],[20],[21]

it was observed that the change in molar ratio of Si/Ti did not cause any significant change to the band gap energy.

Functional Group Analysis

The functional group analysis of the prepared photocatalysts is presented by the FTIR spectra in Figure 4. The broad peak present on sample WO_3-TiO_2 at the region around 450 – 800 cm^{-1} corresponded to the overlapping of Ti-OH and Ti-O-Ti peaks [18]-[21],[23]. Meanwhile, the intense bands observed at region *ca.* 3448 cm^{-1} and 1650 cm^{-1} were attributed to the OH group due to water adsorption on the surface of the samples that occurred during the sol-gel treatment [18]-[21],[23]. For TUD-C, the successful formation of TUD-C can be observed via the appearance of bands at 1100 cm^{-1} and 464 cm^{-1}, which are attributed to the Si-O-Si asymmetric stretching and vibration of T-O-T bond, respectively [18]-[19],[23]. Furthermore, the small peak at *ca.* 557 cm^{-1} is attributed to MFI phase skeleton vibration [18]-[19],[23], while the peak at 1237 cm^{-1} has corresponded to the TO_4 tetrahedral structure of the zeolitic functional group of ZSM-5 [18]-[19],[23]. Upon successful loading of WO_3-TiO_2 into TUD-C, the intensity of zeolites peaks reduced, suggesting the silica system was influenced by Ti due to the possibility of the formation of Ti-O-Si linkage instead of Si-O-Si [18]-[19],[23].

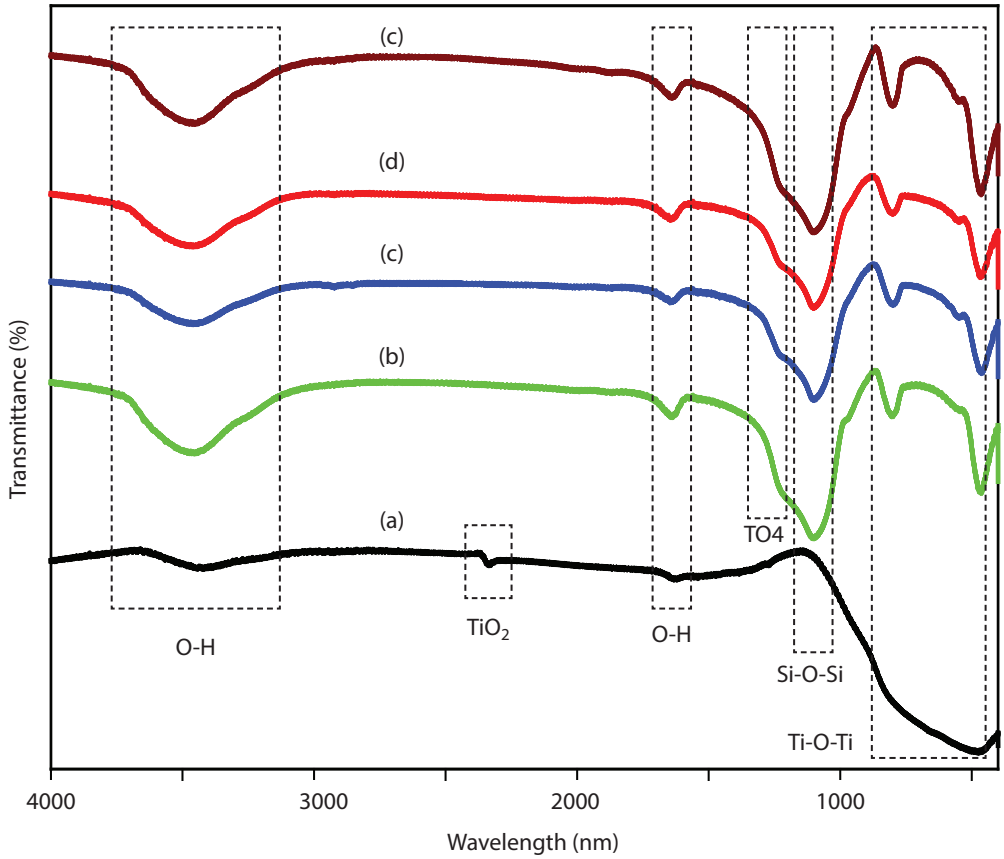

Figure 4 FTIR spectra of (a) WO_3-TiO_2, (b) TUD-C, (c) WO_3-TiO_2/TUD-C (10), (d) WO_3-TiO_2/TUD-C (30) and (e) WO_3-TiO_2/TUD-C (50)

Textural Analysis

Figure 5 shows the isotherms of WO_3-TiO_2, TUD-C, WO_3-TUD-C/TiO_2 (10), WO_3-TUD-C/TiO_2 (30), WO_3-TUD-C/TiO_2 (50). It was found that all the prepared samples showed the type (IV) isotherm with hysteresis type H2 except for WO_3-TiO_2, which demonstrated a type H3 hysteresis. The H2 hysteresis loop indicated that the narrow neck shape of porous was formed, while H3 hysteresis loop indicated the formation of the non-uniform size of slit shape pores [25].

The pore size distribution for the prepared samples, as presented in Figure 6 was analysed via Barrett-Joyner-Halenda (BJH) analysis. From the figure, it was found that sample WO_3-TiO_2 (a) demonstrated a wide pore size distribution while the samples WO_3-TiO_2/TUD-C (c-e) revealed a narrow distribution of pore size ranging between 7 – 13 nm, suggesting the successful formation of the sample with uniform porosity and the presence of mesoporosity. The values of the surface area (SA), pore diameter (PD) and pore volume (PV) are tabulated in Table 2. The specific surface area was calculated by using Brunauer, Emmett and Teller (BET) method. In accordance with the obtained surface area, WO_3-TiO_2 showed the lowest surface area values (8.4 m^2/g) while TUD-C demonstrated the highest surface area (199.6 m^2/g). Compared to TUD-C, the surface area decreased after loading of WO_3-TiO_2, suggesting the well-dispersion of WO_3-TiO_2 in the pores of TUD-C. This phenomenon was also in agreement with the XRD patterns of WO_3-TiO_2 which its crystallinity decreased compared to TiO_2. On the other hand, the pore volume of the photocatalyst increased significantly upon the incorporation of WO_3-TiO_2 into TUD-C. For example, the pore volume of WO_3-TiO_2/TUD-C (10) (Entry 2) was increased to 0.41 cm^3/g compared to 0.04 cm^3/g for WO_3-TiO_2 (Entry 1). However, increasing the molar ratio of Si/Ti from 30 (Entry 3) to 50 (Entry 4) demonstrated a slight increase in pore volume from 0.50 to 0.53 cm^3/g. In addition, the pore diameter of WO_3-TiO_2 (Entry 1) increased from 3.89 nm to 10.27 nm when TUD-C with molar ratio Si/Ti (10) was loaded (Entry 2). However, increasing the molar ratio of Si/Ti to 30 (Entry 3) showed

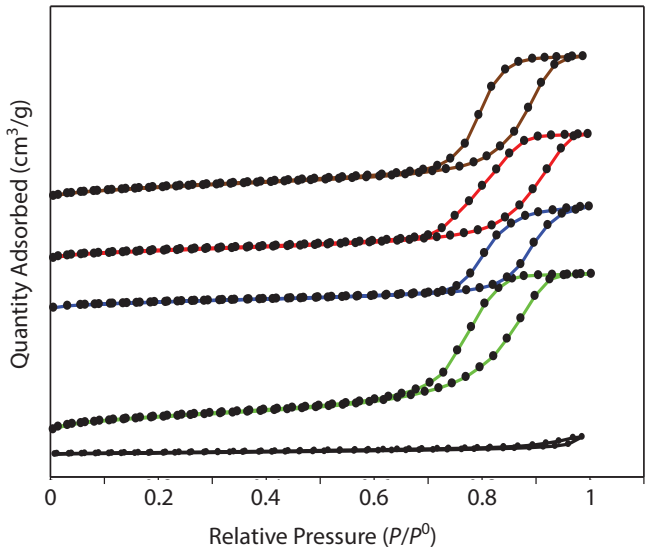

Figure 5 N_2 adsorption-desorption isotherms of (a) WO_3-TiO_2, (b) TUD-C, (c) WO_3-TiO_2/TUD-C (10), (d) WO_3-TiO_2/TUD-C (30) and (e) WO_3-TiO_2/TUD-C (50). The enlarged isotherm of sample (a) can be found in Figure 7

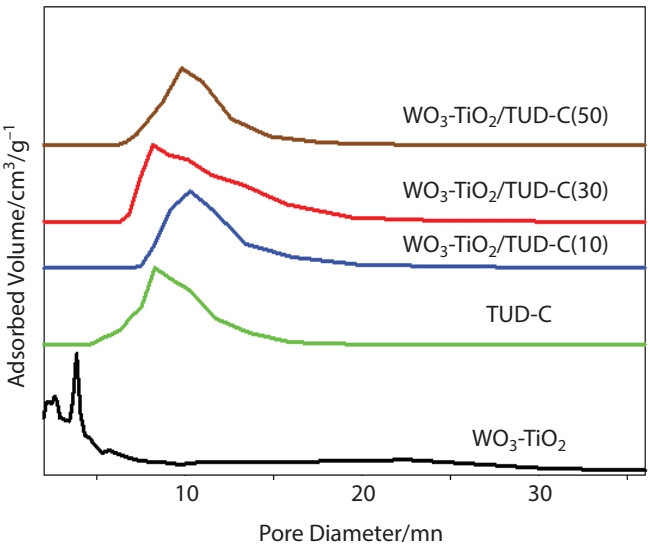

Figure 6 Pore size distributions of (a) WO_3-TiO_2, (b) TUD-C, (c) WO_3-TiO_2/TUD-C (10), (d) WO_3-TiO_2/TUD-C (30) and (e) WO_3-TiO_2/TUD-C (50)

Table 2 The values of surface area, pore diameter and pore volume of the prepared samples

Entry	Sample	Surface area ($m^2 g^{-1}$)	Pore diameter (nm)	Pore volume ($cm^3 g^{-1}$)
1	WO_3-TiO_2	8.4	3.89	0.04
2	WO_3-TiO_2/TUD-C(10)	119.6	10.27	0.41
3	WO_3-TiO_2/TUD-C(30)	139.3	8.16	0.50
4	WO_3-TiO_2/TUD-C(50)	149.4	16.74	0.53
5	TUD-C	199.6	8.27	0.04

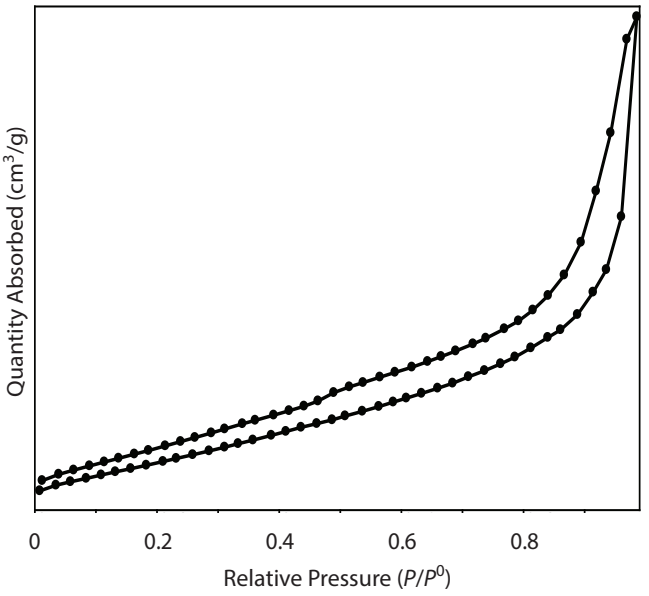

Figure 7 N_2 adsorption-desorption isotherm of sample WO_3-TiO_2

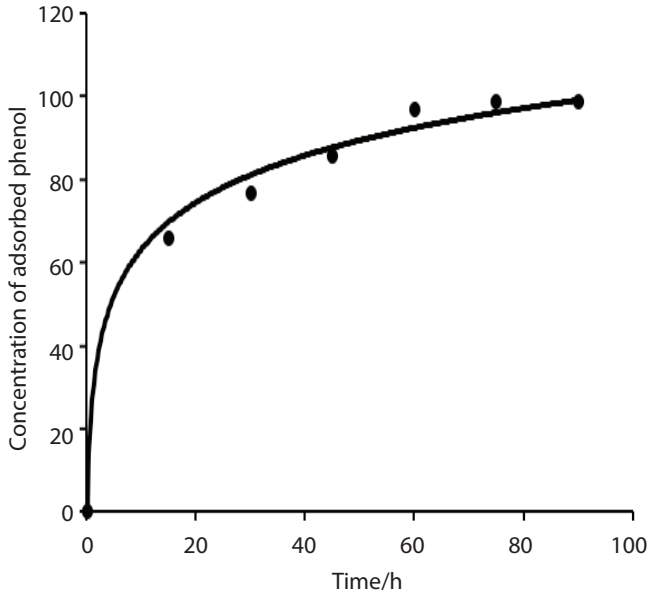

Figure 8 Adsorption of phenol in dark condition of sample TUD-C

a decrease in pore diameter value. This phenomenon could be due to the accretion of WO-TiO_2 on the pore month of TUD-C, resulting in the reduction of pore radius. [28]. Further increase in the molar ratio of Si/Ti to 50 (Entry 4) demonstrates the increase in pore diameter to 16.74 nm. For comparison, the value of pore volume and pore diameter for unmodified TUD-C are also listed in Table 2.

Photocatalytic Testing

The photocatalytic efficiency of the prepared WO_3-TiO_2/TUD-C series was evaluated by removing methylene blue under UV light irradiation for 1 h. Prior to the photocatalytic reaction, the adsorption test was performed under dark conditions for 1 h to achieve equilibrium and the adsorption results are shown in Figure 8. The photocatalytic performance of photocatalysts is presented in Figure 9. For comparison, the photocatalytic activity of TUD-C was also evaluated and its photocatalytic activity was found to be 42%. Since TiO_2 was absent, the results suggested that the degradation of MB was associated with the catalytic activity of TUD-C. It was reported that the presence of Brønsted acid sites within its zeolitic structure of TUD-C were active sites for the degradation [18].

In addition, It was observed that the photocatalytic activity was significantly increased from 18% for WO_3-TiO_2 to 52% for WO_3-TiO_2/TUD-C(10), respectively. The increased photocatalytic activity would be mainly due to the increase in the surface area, thus providing more active sites for reaction to occur [26],[27]. The highest photocatalytic activity was achieved on sample WO_3-TiO_2/TUD-C(30) as up to 68% of methylene blue was degraded. Increasing Si/Ti molar ratio to 50 (WO_3-TiO_2/TUD-C(50) caused a slight decrease in activity as up to 58% of methylene blue was degraded. It is suggested that the optimum molar ratio of Si/Ti was found to be 30. The increase of the molar ratio of Si/Ti would cause the trapping of WO_3-TiO_2 in the excess silica matrix, thus causing loss of the active sites at the surface for an effective photocatalytic reaction. On the other hand, when the molar ratio of Si/Ti was smaller than 30, the amount of TUD-C would be insufficient for the good distribution of WO_3-TiO_2, thus leading to the aggregation of WO_3-TiO_2. As a result, photocatalytic activity decreased. This finding was also in agreement with a previous work that claimed that the aggregation of photocatalyst might occur when the amount of support (TUD-C) was low [17].

Morphological Studies

Since the WO_3-TiO_2/TUD-C(30) sample gave the highest photocatalytic activity, further investigation was performed to investigate the morphological properties of the sample. As shown in Figure 10, the

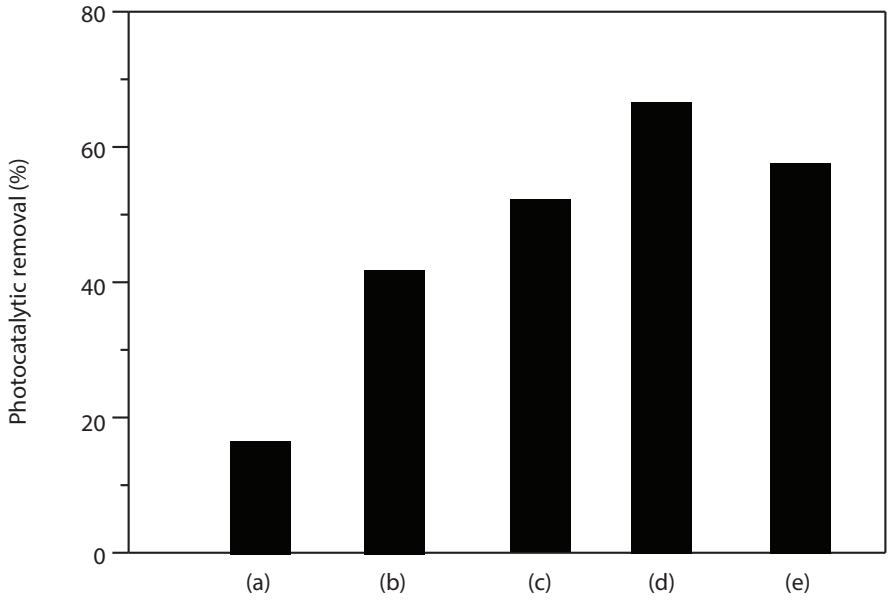

Figure 9 Photocatalytic removal of methylene blue under UV light irradiation for 1 h using (a) WO_3-TiO_2, (b) TUD-C, (c) WO_3-TiO_2/TUD-C(10), (d) WO_3-TiO_2/TUD-C(30), (e) WO_3-TiO_2/TUD-C(50)

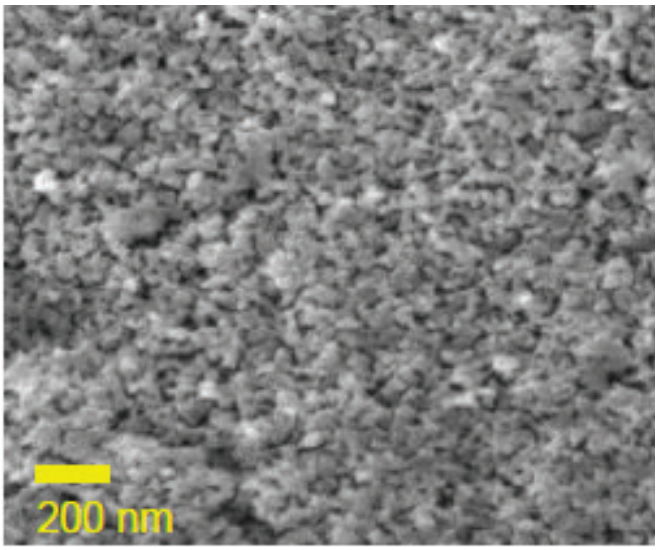

Figure 10 FESEM image of WO_3-TiO_2/TUD-C(30)

sample demonstrated a uniform size of crystallite in nanoscale. In addition, the successful formation of WO_3-TiO_2 was confirmed using EDX mapping analysis, as shown in Figure 11. It was observed that the WO_3-TiO_2 was well-distributed on the TUD-C. Therefore, it can be suggested that no agglomeration and aggregation of WO_3-TiO_2 on TUD-C support, thus contributed to the high photocatalytic activity.

CONCLUSION

A series of mesoporous WO_3-TiO_2 supported TUD-C was successfully prepared using a sol-gel technique with different molar ratios of Si/Ti (10, 30 and 50). The formation of mesoporosity was achieved by a one-step single soft-template approaching using triethanolamine and tetraethylammonium hydroxide

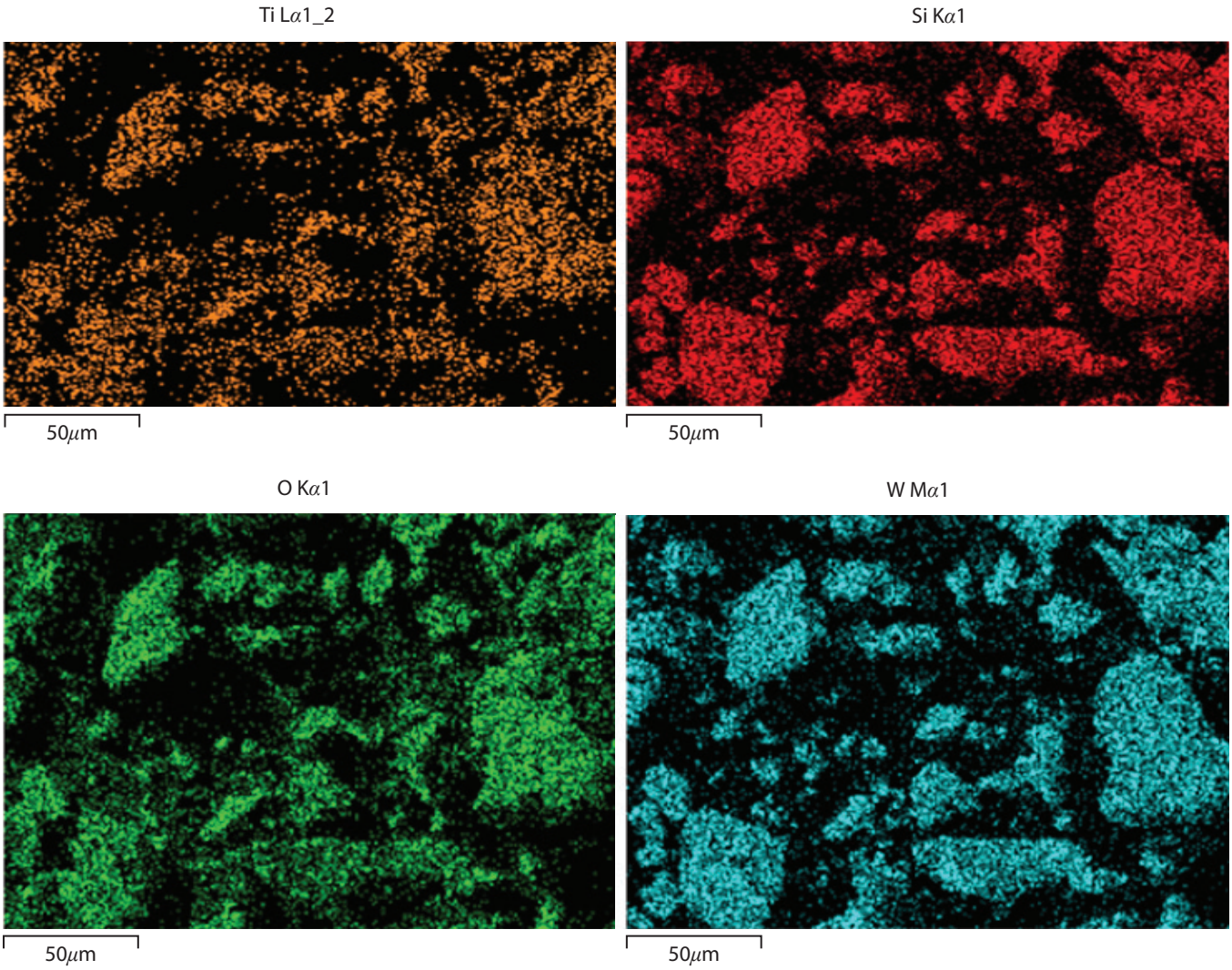

Figure 11 EDX mapping for elements present in WO_3-TiO_2/TUD-C(30)

as scaffolding agent. The photocatalytic performance of WO_3-TiO_2 was significantly improved with the loading onto TUD-C support, suggesting that the TUD-C has promising support for photocatalytic reaction. The highest photocatalytic activity was achieved on sample WO_3-TiO_2 on TUD-C(30) under UV light irradiation in 1 h. It was concluded that the high surface area with mesoporous structure, high crystallinity, and uniform distribution of WO_3-TiO_2 on the TUD-C support contributed to the high photocatalytic activity.

ACKNOWLEDGEMENT

The authors are grateful to the Ministry of Higher Education (MOHE), Malaysia and Universiti Teknologi Malaysia (UTM) for the financial support given under UTM High Impact Research Grant (Cost Center No. Q. J130000.2454.08G53).

REFERENCES

[1] R. Geetam, & A. Kumar, "Fabrication and characterization of mixed dye: Natural and synthetic organic dye", *Optical Materials,* 79, pp. 296-301, 2018.

[2] E. S. B. Ferreira, A. N. Hulme, H. McNab, & A. Quye, "The natural constituents of historical textile dyes", *Chemical Society Reviews*, 33, 6, pp. 329-336, 2004.

[3] S. Gita, A. Hussan, & T. G. Choudhury, "Impact of textile dyes waste on aquatic environments and its treatment", *Environ. Ecol*, 35, 3C, pp. 2349–353, 2017.

[4] B. Malini & G. A. Gnana, "Journal of Environmental Chemical Engineering C, N and S-doped TiO_2-characterization and photocatalytic performance for rose bengal dye degradation under day light", *Journal Environmental. Chemical. Engineering*, 6, 5, pp. 5763–770, 2018.

[5] Y. C. Wong, Y. S. Szeto, W. H. Cheung, & G. McKay, "Adsorption of acid dyes on chitosan equilibrium isotherm analyses", *Process. Biochem*, 39, 6, pp. 695–704, 2004.

[6] I. A. W. Tan, A. L. Ahmad, & B. H. Hameed, "Adsorption of basic dye on high-surface area activated carbon prepared from coconut husk: Equilibrium, kinetic and thermodynamic studies", *Journal of Hazard. Materials*, 154, 1-3 pp. 337–346, 2008.

[7] T. R. Bastami, S. Khaknahad, & M. Malekshahi, "Sonochemical versus reverse-precipitation synthesis of Cu_xO/Fe_2O_3/MoC nano-hybrid: removal of reactive dyes and evaluation of smartphone for colorimetric detection of organic dyes in water media", *Environmental Science and Pollution Research*, 27, 9, pp. 9364–381, 2020.

[8] A. H. Jawad, N. N. A. Malek, A. S. Abdulhameed, & R. Razuan, "Synthesis of magnetic chitosan-fly ash/Fe3O4 composite for adsorption of reactive orange 16 dye: Optimization by box–Behnken design", *Journal Polymers and the Environment*, 28, 3, pp. 1068–082, 2020.

[9] X. Zhao, X. Wang, G. Song, & T. Lou, "Microwave assisted copolymerization of sodium alginate and dimethyl diallyl ammonium chloride as flocculant for dye removal", *Int. J. Biol. Macromol*., 156, pp. 585–590, 2020.

[10] G. Crini & E. Lichtfouse, "Advantages and disadvantages of techniques used for wastewater treatment" *Environmental Chemistry Letters*, 17, 1, pp. 145–155, 2019.

[11] D. Ghime & P. Ghosh, "Advanced oxidation processes: A powerful treatment option for the removal of recalcitrant organic compounds", *Advanced Oxidation Processes - Applications, Trends, and Prospects*, IntechOpen, 2020.

[12] M. Luo, D. Bowden, & P. Brimblecombe, "Removal of dyes from water using a TiO2 photocatalyst supported on black sand" *Water, Air, and Soil Pollution*, 198, 1, pp. 233–241, 2009.

[13] H. Yan, X. Wang, M. Yao, & X. Yao, "Band structure design of semiconductors for enhanced photocatalytic activity: The case of TiO2", *Progress Natural Science: Materials International*, 23, 4, pp. 402–407, 2013.

[14] F. Mirante et al., "Mesoporous nanosilica-supported polyoxomolybdate as catalysts for sustainable desulfurization", *Microporous Mesoporous Materials*, 275, pp. 163–171, 2019.

[15] J. Ye, X. Li, J. Hong, J. Chen, & Q. Fan, "Photocatalytic degradation of phenol over ZnO nanosheets immobilized on montmorillonite" *Materials Science in Semiconductor. Processing*, 39, pp. 17–22, 2015.

[16] J. Zhou, Z. Hua, J. Shi, Q. He, L. Guo, & M. Ruan, "Synthesis of a hierarchical micro/mesoporous structure by steam-assisted post-crystallization", *Chemistry*, 15, 47, pp. 12949–12954, 2009.

[17] M. S. Hamdy, "Au-TUD-1: A new catalyst for aerobic oxidation of cyclohexene", *Microporous Mesoporous Mater.*, 220, pp. 81–87, 2016.

[18] Y. K. Ooi, F. Hussin, L. Yuliati, & S. L. Lee, "Comparison study on molybdena-titania supported on TUD-1 and TUD-C synthesized via sol-gel templating method: Properties and catalytic performance in olefins epoxidation", *Materials Research Express*, 6, 7, p. 074001, 2019.

[19] Y. K. Ooi, Y. Leny, & S. L. Lee, "Cr doped TiO_2 supported photocatalyst for dye photodegradation", *Jurnal Teknologi*, 69, 5, pp. 81–86, 2014.

[20] P. W. Koh, M. H. M. Hatta, S. T. Ong, L. Yuliati, & S. L. Lee, "Photocatalytic degradation of photosensitizing and non-photosensitizing dyes over chromium doped titania photocatalysts under visible light", *Journal Photochemistry and Photobiology. A Chemistry*, vol. 332, pp. 215–223, 2017.

[21] P. W. Koh, L. Yuliati, & S. L. Lee, "Kinetics and optimization studies of photocatalytic degradation of methylene blue over Cr-doped TiO_2 using response surface methodology", *Iran. Journal Science Technology. Transactions. A Science*, 43, 1, pp. 95–103, 2019.

[22] W. Yao, H. Fang, E. Ou, J. Wang, & Z. Yan, "Highly efficient catalytic oxidation of cyclohexane over cobalt-doped mesoporous titania with anatase crystalline structure", *Catalysis Communications*, 7, 6, pp. 387–390, 2006.

[23] C. M. Ling, L. Yuliati, H. O. Lintang, & S. L. Lee, "TUD-C-supported tungsten oxide-doped titania catalysts for cyclohexane oxidation", *Malaysian Journal Chemistry*, 22, 2, pp. 29-36, 2020

[24] Y. Nakasaka, J.-I. Nishimura, T. Tago, & T. Masuda, "Deactivation mechanism of MFI-type zeolites by coke formation during n-hexane cracking", *Chemistry Engineering Journal*, 278, pp. 159–165, 2015.

[25] K. A. Cychosz & M. Thommes, "Progress in the physisorption characterization of nanoporous gas storage materials", *Engineering*, 4, 4, pp. 559–566, 2018.

[26] Y. K.Ooi, L.Yuliati, D. Hartanto, H.Nur, & S. L. Lee, "Mesostructured TUD-C supported molybdena doped titania as high selective oxidative catalyst for olefins epoxidation at ambient condition", *Microporous and Mesoporous Materials*, 225, pp. 411-420, 2016.

[27] M. H. M. Hatta, H. O. Lintang, S. L. Lee, and L. Yuliati, "Synthesis of highly active crystalline carbon nitride prepared in various salt melts for photocatalytic degradation of phenol", *Turkish Journal of Chemistry*, 43, 1, pp. 63–72, 2019.